Available free online at www.medjchem.com

Mediterranean Journal of Chemistry

Mediterranean Journal of Chemistry **2019**, 7(6), 416-422

Elaboration and structural characterization of phosphate glasses with composition $37.5Na_2O$-$25[(1-x)MgO$-$xNiO]$-$37.5P_2O_5$ ($0 \leq x \leq 1$)

Laila Lamrous [1], Redouane Farid [1], Abdelaziz El Jazouli [1,*], Saida Krimi [2,*], Mustapha Haddad [3], Hassane Oudadesse[4], Said Sebti [1] and Michel Couzi [5]

[1] Hassan II University of Casablanca, Faculty of Sciences Ben M'sik, Chemistry Department, LCMS/LCPCE – URAC17, BP 7955, 20702 Casablanca, Morocco

[2] Hassan II University of Casablanca, Faculty of Sciences Ain chock, Chemistry Department, LPCMI, B. P. 5366 Maarif 20000, Morocco

[3] Laboratoire de Spectrométrie des Matériaux et Archéomatériaux (LASMAR), URAC 11, Université Moulay Ismail, Faculté des Sciences, B.P 11201 Zitoune, Meknes 50000, Morocco

[4] Univ Rennes, CNRS, ISCR-UMR 6226, F-35000 Rennes, France

[5] Université de Bordeaux, Institut des Sciences Moléculaires, CNRS UMR 5255, Talence cedex, France

Abstract: Phosphate glasses, with molar compositions $37.5Na_2O$-$25[(1-x)MgO$-$xNiO]$-$37.5P_2O_5$ ($0 \leq x \leq 1$), have been prepared using the conventional melt quenching technique. The free nickel glass is colorless while the glasses containing nickel are yellow. The effect of Ni^{2+} ions on structural and physico-chemical properties of these glasses has been investigated by XRD, DTA, EPR, Raman, FTIR spectroscopies and by density and chemical durability measurements. Substitution of Ni^{2+} for Mg^{2+} strengthens the glass network, as shown by the decrease of the molar volume, the increase of the glass transition temperature, and the improvement of the chemical durability. This behavior is a consequence of the replacement of Mg-O bonds by more covalent Ni-O bonds. The glass structure consists of tri-phosphate $(P_3O_{10})^{5-}$ and di-phosphate $(P_2O_7)^{4-}$ groups, and Mg/NiO_6 octahedra, with Mg-O-P and Ni-O-P linkages.

Keywords: NaMg/Ni-Phosphate glasses, Raman/FTIR, EPR, Chemical durability.

Introduction

Phosphate glasses are of great interest because of their physical and chemical properties, such as optical devices [1,2], waveguides [3] and glass to metal seals [4]. Also, the phosphate glasses become particularly attractive in the medical field for their poor durability. Indeed, the solubility of phosphate glasses can be used to create bioactive materials [5-7]. The diverse properties and applications of phosphate glasses depend on their structure, which is based on the distribution of Q^n tetrahedral units in the vitreous network (n varies from 0 to 3 and represents the number of bridging oxygen per PO_4 tetrahedron). The connection of PO_4 tetrahedra gives rise to different phosphate groups depending on the value of O/P ratio. So, the glass structure can be formed by a cross-linked network of Q^3 tetrahedra (vitreous P_2O_5, O/P = 2.5), infinite metaphosphate chains of Q^2 tetrahedra (vitreous $NaPO_3$, O/P = 3), or by small diphosphate $P_2O_7^{2-}$ (Q^1, O/P = 3.5) and monophosphate PO_4^{3-} (Q^0, O/P = 4) anions [8].

Phosphate glasses containing Mg^{2+} or Ni^{2+} ions have been investigated, and the number coordination of these ions was found to be six [9,10]. The average Ni-O distance in $(NaPO_3)_{1-x}(NiO)_x$ ($0.008 \leq x \leq 0.30$) glasses is 2.06 Å[10]. Infrared and Raman spectra of $(50-x/2)Na_2O$–$xMgO$–$(50-x/2)P_2O_5$ [$(100-x)NaPO_3$-$xMgO$] ($0 \leq x \leq 42.8$ mol%, $3 \leq O/P \leq 3.75$) glasses have been reported by Oueslati et al [11]. The composition x = 0 ($NaPO_3$, O/P = 3) corresponds to the metaphosphate characterized by infinite linear chains where each PO_4 tetrahedron shares two oxygen atoms (Q^2) with two other PO_4 tetrahedra. Addition of MgO content induces an evolution of structural units from Q^2 (metaphosphate chains) to Q^1 (P_2O_7 diphosphate groups) and Q^0 (PO_4 monophosphate groups) indicating the depolymerization of phosphate chains [11]. This series includes the triphosphate composition $37.5Na_2O$-$25MgO$-$37.5P_2O_5$ ($Na_3MgP_3O_{10}$, O/P = 3.33). We focus our present investigation on this composition, due to the importance of the triphosphate groups (P_3O_{10}) in biological and medical applications [12,13].

*Corresponding author : Abdelaziz El Jazouli, Saida Krimi
Email address : eljazouli_abdelaziz@yahoo.fr, krimisaida@yahoo.fr
DOI:

Received November 5, 2018
Accepted November 28, 2018
Published December 15, 2018

We can cite the role of the adenosine triphosphate (ATP) in the biochemistry of all known living beings. ATP provides the energy needed for chemical reactions of metabolism, locomotion, cell division, or the active transport of chemical species across biological membranes. To release this energy, ATP molecule is cleaved, by hydrolysis, into adenosine diphosphate (ADP). The cells then regenerate ATP from ADP. It is also known that the introduction of paramagnetic transition ions, such as Mn^{2+}, Ni^{2+}, and Cu^{2+}, in compounds induces photoluminescence and improves catalytic properties [14,15]. The present work concerns a new series of mixed Mg-Ni-phosphate-based glasses $37.5Na_2O$-$25[(1-x)MgO$-$xNiO]$-$37.5P_2O_5$ ($Na_3Mg_{1-x}Ni_xP_3O_{10}$), $0 \leq x \leq 1$. It reports their synthesis method and their characterization by X-ray diffraction (XRD), differential thermal analysis (DTA), electronic paramagnetic resonance (EPR), Raman, Fourier transform infrared (FTIR) spectroscopies and by density and chemical durability measurements.

Experimental and characterization

Synthesis

Glass samples with chemical formula $37.5Na_2O$-$25[(1-x)MgO$-$xNiO]$-$37.5P_2O_5$ ($0 \leq x \leq 1$) were prepared in the air by the conventional melt quenching technique. Sodium carbonate (Na_2CO_3, 99,4 %), magnesium oxide (MgO, 99.5%), nickel oxide (NiO, 99. 8%), and ammonium di-hydrogen phosphate ($NH_4H_2PO_4$, 99,5%) were used as starting materials. The mixtures, corresponding to the desired compositions, were initially heated in a platinum crucible at 200°C, 400°C and 600°C for 12 h to decompose reagents. The temperature was then progressively put to 950°C and held constant at this value for 15 min. The liquid was then poured on a metallic plate preheated at 150°C, to avoid the thermal shock and the break of glasses. Before characterization, all glasses were annealed at (T_g-20) °C to eliminate residual stresses. Fig.1 shows photographs of the glasses prepared under the conditions above, and the corresponding powders obtained by grinding pieces of glasses. The free nickel glass (x = 0) is colorless while glasses containing nickel are yellow-brown.

Composition	x = 0	x = 0.25	x = 0.5	x = 0.75	x = 1
Glass	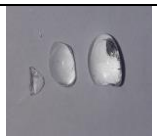	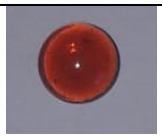	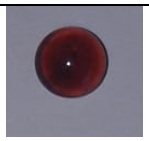		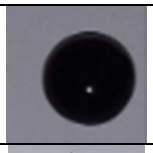
Powder			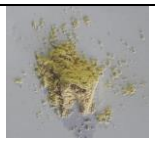		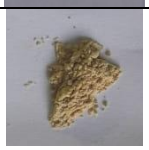

Figure 1. Photographs of $37.5Na_2O$-$25[(1-x)MgO$-$xNiO]$-$37.5P_2O_5$ ($0 \leq x \leq 1$) glasses and powders obtained by grinding pieces of glasses.

Characterization

XRD measurements were done at room temperature with a powder diffractometer (Advance D8) using Cu Kα radiation. Data were collected in the 2θ range of 10-60° with a step of 0.02 and a count time of 12s. Glass transition and crystallization temperatures (T_g, T_c) were measured on 22–35 mg of samples using the DTG-60H with a heating rate of 10 °C/min, in a platinum crucible. The density (ρ) was measured on bulk glasses by the Archimedes method, using diethyl phthalate as the immersion liquid. It was calculated from the following relation: $\rho = [m_1/(m_1-m_2)]\ \rho_0$, where m_1 is the mass of the sample in air, m_2 the mass of sample immersed in the diethyl phthalate and ρ_0 the density of the diethyl phthalate at room temperature. Three measurements were made for each glass. The average values are reported Table 1. The accuracy of measurements is about ± 0.03 g/cm^3. The molar volume was calculated from the relation: $V_m = M/\rho$ (M is the molar mass of the glass). Raman spectra were carried out using a spectrometer LabRam HR Evolution - Horiba Scientific, with a laser source (λ= 532 nm) under the confocal microscope with an X50 objective and power to sample 8 mW. FTIR spectra were recorded on an Equinox 55 Spectrometer in the frequency range 400 - 4000 cm^{-1} with a resolution of 2 cm^{-1}. Glass powder was mixed and ground with KBr (potassium bromide) in a Glass/KBr mass ratio of 1/200. This mixture is then compressed to form a translucent pastille to be placed in the IR beam. EPR spectra were recorded at room temperature, using a Bruker spectrometer, working in X band, with a frequency of 9.788 GHz. Chemical durability tests were carried out on bulk samples using distilled water at 90°C. The weight loss was measured after 24, 48, 96, 158, and 230 hours of immersion. The dissolution rate of the glasses (ΔR) was calculated from the relationship: $\Delta R = \Delta m/S\ t$, (Δm: weight loss, S: glass surface, t: time).

Results and discussion

XRD, density and molar volume

Table 1 presents the major interesting measured properties for $37.5Na_2O$-25[(1-x)MgO-xNiO]-$37.5P_2O_5$ ($0 \leq x \leq 1$) glasses. Their X-ray diffraction patterns (Fig. 2a) indicate an amorphous state for all compositions. Fig. 2b shows XRD patterns of compounds obtained, after heating the glasses at T_c (°C) for 12 h. The values of T_c (Table 1) were determined by DTA. Crystallization of these glasses leads to the formation of both $NaPO_3$ (ASTM powder diffraction data file, N° 00-01-0648) and $Na_3NiP_3O_{10}$ (ASTM powder diffraction data file, N° 00-030-1225) crystalline phases with some unidentified peaks. The peaks observed in the glass spectrum of free nickel composition (x = 0: $Na_3MgP_3O_{10}$) do not correspond to any known crystalline phase in the base of X-ray data. Fig. 3 shows the variation of the density (ρ) and the molar volume (V_m) versus NiO content of glasses. The replacement of MgO by NiO induces an increase of density due to the molecular weight of NiO (M_{NiO} = 74.7g/mol) higher than that of MgO (M_{MgO} = 40.3 g/mol). The decrease of the molar volume (Table 1), is because the ionic radius of Ni^{2+} ions (0.69Å) is lower than that of Mg^{2+} ions (0.73 Å). This decrease of molar volume indicates that Ni^{2+} ions reticulate the vitreous network suggesting the increase in the rigidity of the structure and formation of Ni-O-P linkage more covalent than Mg-O-P one. Indeed, the evolution of the molar volume, as a function of the oxide content introduced into the glass, reflects the effect of this oxide within the vitreous network: i) if the molar volume remains constant, the introduced cations are placed in the interstitial sites of the glass network, as observed in ZnO-$NaPO_3$ glasses [16]; ii) a decrease in V_m shows that the introduced cations reinforce the glass network which becomes more rigid; as observed in Na_2O-MO-P_2O_5 (M = Mg, Mn, Cu, Zn) glasses [10,17-19]; iii) an increase in V_m is indicative of an expansion of the network, this case has been observed in $50P_2O_5$-(50-x)Na_2O-xCaO glasses [20].

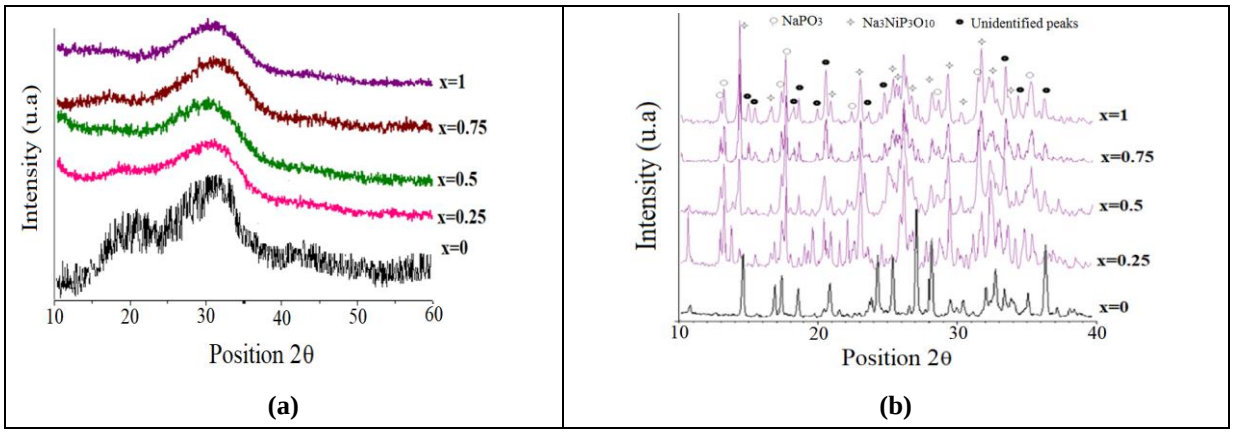

Figure 2. X ray diffraction of (a) $37.5Na_2O$-25[(1-x)MgO-xNiO]-$37.5P_2O_5$ ($0 \leq x \leq 1$) glasses and of (b) compounds obtained after heating these glasses at T_c, for 12 hours.

Differential thermal analysis

Fig. 4 shows DTA curves of $37.5Na_2O$-25-[(1-x)MgO-xNiO]-$37.5P_2O_5$ (x = 0, 0.5, 1) glasses. The value of T_g (Table 1) increases from 364 °C for x = 0 to 417 °C for x = 1, which implies that substitution of Ni^{2+} ions for Mg^{2+} ions strengthens the vitreous network, in good agreement with the decrease, observed previously for the molar volume. This increase of T_g can be explained by the high field strength, ΔF (ΔF = z/r^2; with z is the valence cation, and r is the ionic radius) of Ni^{2+} (4.2 A^{-2}) compared to that of Mg^{2+} (3.86 A^{-2}).

Table 1. Nominal molar compositions, molar mass (M), density (ρ), molar volume (V_m) and characteristic temperatures (T_g, T_c) of $37.5Na_2O$-25[(1-x)MgO-xNiO]-$37.5P_2O_5$ ($0 \leq x \leq 1$) glasses.

Molar composition (%mol)				Molar mass	ρ	V_m	T_g	T_c
Na_2O	MgO	NiO	P_2O_5	(g/mol)	(± 0.03 g/cm^3)	(cm^3/mole)	(± 5 °C)	(± 5 °C)
37.5	25	0	37.5	86.55	2.55	33.9 ± 0.4	364	500
37.5	18.75	6.25	37.5	88.70	2.79	31.8 ± 0.3	390	502
37.5	12.5	12.5	37.5	90.85	3.12	29.1 ± 0.3	393	486
37.5	6.25	18.75	37.5	92.99	3.33	27.9 ± 0.3	415	521
37.5	0	25	37.5	95.14	3.90	24.4 ± 0.2	418	523

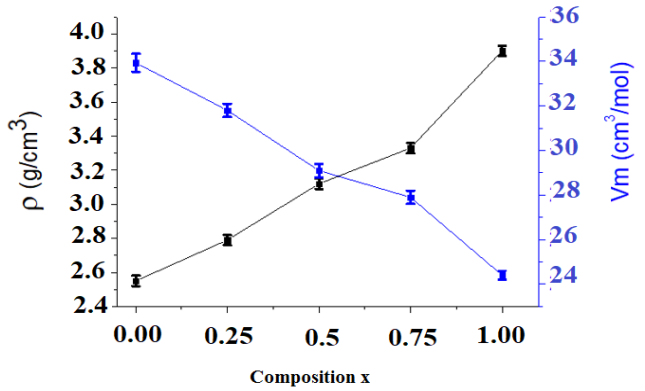

Figure 3. Evolution of density and molar volume for $37.5Na_2O$-$25[(1-x)MgO$-$xNiO]$-$37.5P_2O_5$ ($0 \leq x \leq 1$) glasses versus NiO mol%.

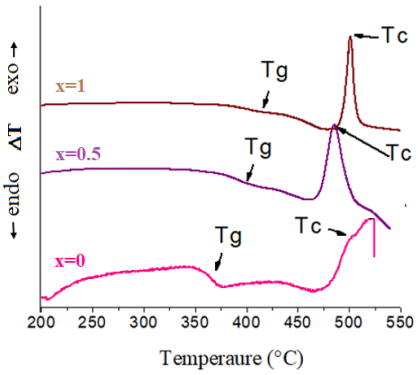

Figure 4. DTA thermograms for $37.5Na_2O$-$25[(1-x)MgO$-$xNiO]$-$37.5P_2O_5$ ($0 \leq x \leq 1$) glasses.

EPR spectroscopy

EPR technique is an indirect method for the study of glass structure with transition metal ions as paramagnetic probes. We use this technique to check the oxidation number of nickel ions and to have information on the sites they occupy in the glass structure. EPR spectrum of $37.5Na_2O$-$12.5MgO$-$12.5NiO$-$37.5P_2O_5$ glass (x = 0.5), recorded at room temperature, is shown in Fig. 5. It exhibits three lines centred at g ≈ 2.0, 2.2 and 4.3. It is known that 3d transition elements as Co and Ni introduced in glasses often contain iron impurities. Moreover, Fe^{3+} ion is very sensitive to EPR. The signal at g ≈ 4.3 is associated to isolated Fe^{3+} ions at the rhombic site; the other one at g ≈ 2.0 is assigned to two or more Fe^{3+} ions coupled together, as clusters in the glass structure, with Fe^{3+}-Fe^{3+} interaction [21,22]. The value of the signal at g ≈ 2.2 is close to those obtained, at room temperature, for Ni^{2+} doped sodium phosphate glasses Na_2O-P_2O_5: Ni^{2+} (g = 2.28) and Ni^{2+} doped perovskite $YAlO_3$: Ni^{2+} (g = 2.16) [23,24]. It is attributed to Ni^{2+} ions in octahedral sites.

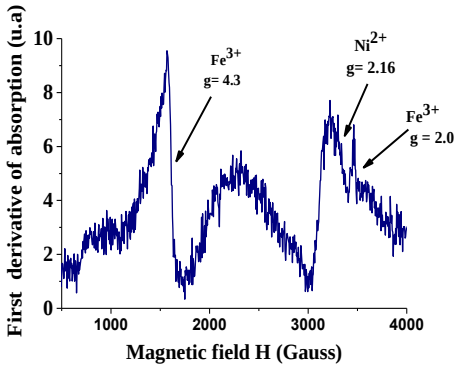

Figure 5. EPR spectrum of $37.5Na_2O$-12.5 MgO-$12.5NiO$-$37.5P_2O_5$ glass recorded at room temperature.

Infrared and Raman spectroscopies

FTIR and Raman spectra of $37.5Na_2O$-25-$[(1-x)MgO$-$xNiO]$-$37.5P_2O_5$ ($0 \leq x \leq 1$) glasses (Fig. 6) have similar shapes and show broad bands characteristic of the structural disorder of glasses. Band wave numbers and their assignments are reported in Table 2. Raman and FTIR spectra for the free nickel composition (x = 0) are similar to those reported by Oueslati et al. [11]. Raman spectra present a weak band at ~ 1270 cm^{-1}, a very strong and broad band between 1080 and 1200 cm^{-1} with a maximum around 1160 cm^{-1} and a shoulder at ~ 1120, a band with medium intensity around 1040 cm^{-1}, a shoulder at ~ 970 cm^{-1}, a strong and broad band between 650 and 800 cm^{-1} with a maximum at ~ 700 cm^{-1}, a set of bands with low intensity between 450 and 600 cm^{-1}, and a broad band between 250 and 450 cm^{-1} centered at ~ 350 cm^{-1}. FTIR peaks are observed at about, 3450, 1630, 1260, 1140, 1040, 990, 890, 720 and 550 cm^{-1}. The peaks around 1270 cm^{-1} and 1160 cm^{-1} are attributed respectively to the asymmetric stretch ν_{as} (PO_2) and the symmetric stretch ν_s (PO_2) of the two non-bridging oxygen atoms bonded to a phosphorus atom in phosphate tetrahedron [25]. The band at ~ 1040 cm^{-1} is assigned to the symmetric stretch ν_s (PO_3) of PO_3 end groups. Bands observed in 850-990 cm^{-1} and 650-800 cm^{-1} regions are attributed to the asymmetric vibrations ν_{as} (P-O-P) and symmetric stretch ν_s (P-O-P) respectively [26,27]. The bands between 450 and 600 cm^{-1} are attributed

to bending vibrations δ(POP) of phosphate P-O-P bridges. The bands observed in 650-800 and 450-600 regions can also be assigned to vibrations of Ni-O bonds, as reported for $LiNiPO_4$ [28] and R_2BaNiO_5 (R=Y, Ho, Er OR Tm) [29] where Ni^{2+} ions occupy octahedra sites. The broad Raman band centred at ~350 cm^{-1} is assigned to lattice vibrations. The infrared spectra bands observed around 1630 and 3450 cm^{-1} are attributed respectively to O-H bending vibrations and vibrations of H_2O molecules [30]. We notice that some peaks shift toward lower frequencies when Ni^{2+} ions replace Mg^{2+} ions. The IR peak attributed to ν_s (PO_2) shifts from 1144 cm^{-1} for the composition x = 0 ($Na_3MgP_3O_{10}$) to 1112 cm^{-1} for the composition x = 1 ($Na_3NiP_3O_{10}$), the Raman peak assigned to ν_s (PO_3) shifts from 1042 cm^{-1} for x = 0 to 1035 cm^{-1} for x = 1, and the Raman shoulder attributed to ν_{as} (PO_3) moves from 1119 to 1106 cm^{-1}. This result implies that the phosphate units interact with Mg^{2+} and Ni^{2+} ions. As Ni-O bond is more covalent than an Mg-O bond, the antagonistic phosphorus-oxygen bond linked to Ni^{2+} ion (P-O-Ni) is longer than that linked to Mg^{2+} ion (P-O-Mg). This explains the P-O vibration shifts toward low wave numbers, because the vibration frequency of a bond is inversely proportional to its distance.

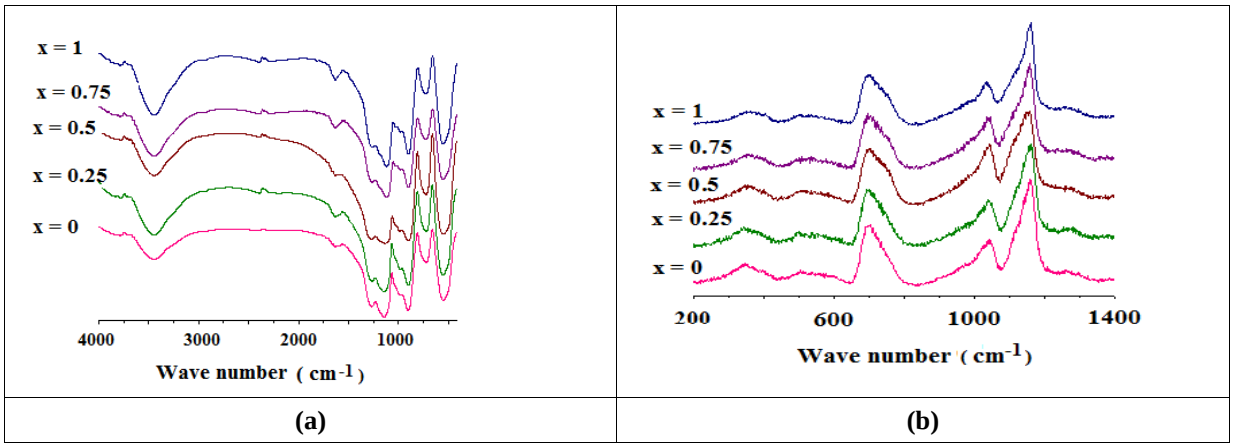

Figure 6. (a) FTIR and (b) Raman spectra of $37.5Na_2O$-25[(1-x) MgO-xNiO]-$37.5P_2O_5$ ($0 \leq x \leq 1$) glasses

Table 2. Raman band assignments of $37.5Na_2O$-25[(1-x)MgO-xNiO]-$37.5P_2O_5$ ($0 \leq x \leq 1$) glasses (w: weak, vw: very weak, m: medium, s: strong, vs: very strong, sh; shoulder).

Wave number (cm^{-1})										Assignment
x = 0		x = 0.25		x = 0.5		x = 0.75		x = 1		
FTIR	Raman	FTIR	Raman	FTIR	Raman	FTIR	Raman	FTIR	Raman	
3459 vs	-	3449 vs	-	3442 vs	-	3439 vs	-	3432 vs	-	ν (O-H)
1627 w	-	1626 w	-	1636 w	-	1636 w	-	1636 w	-	ν (H_2O)
1261 vw	1259 vw	1261 vw	1269 vw	1267 vw	1267 vw	1267 vw	1263 vw	1260 vw	1267 vw	ν_{as} (PO_2)
1144 w	1159 vs (1080-1200)	1140 w	1159 vs (1080-1200)	1134 vw	1158 vs (1080-1200)	1115 w	1157 vs (1080-1200)	1112 w	1157 vs (1080-1200)	ν_s (PO_2)
-	1119 sh	-	1117 sh	-	1110 sh	-	1107 sh	-	1105 sh	ν_{as} (PO_3)
1039 vw	1042 m	1032 vw	1041 m	1032 vw	1040 m	1032 vw	1037 m	1032 vw	1035 m	ν_s (PO_3)
990 vw 894 m	~ 970 sh	990 vw 894 m	~ 970 sh	990 vw 893 w	~ 970 sh	~ 970 sh	~ 970 sh	980 vw 893 m	~ 970 sh	ν_{as} (P-O-P)
720 m	~ 700 s (650-800)	720 m	~ 700 s (650-800)	720 m	~ 700 s (650-800)	720 m	~ 700 s (650-800)	720 m	~ 700 s (650-800)	ν_s (P-O-P) Ni-O (NiO_6)
546 vs	450-600 vw	546 vs	450-600 vw	546 vs	450-600 vw	546 vs	450-600 vw	546 vs	450-600 vw	δ(POP) Ni-O (NiO_6)
-	341 m (250-450)		343 m (250-450)	-	352 m (250-450)		352 m (250-450)	-	353 m (250-450)	Mg-O Lattice vibrations

Chemical durability

The dissolution rate (ΔR) versus NiO content and the weight loss in water solution with time, for $37.5Na_2O$-25[(1-x)MgO-xNiO]-$37.5P_2O_5$ ($0 \leq x \leq 1$) glasses, are shown in Figure 7. The dissolution rate (ΔR) decreases from $3.78.10^{-4}$ g·/cm^2.h to 0.76 10^{-4} g·/cm^2·h, as the NiO is added in the glasses. The weight loss decreases when Ni^{2+} replaces Mg^{2+}. This decrease is due to the increasing number of Ni-O-P more water resistant than Mg-O-P. This result is in good agreement with the decrease of the molar volume and the increase of the glass transition temperature when Ni^{2+} ions are introduced in the glasses.

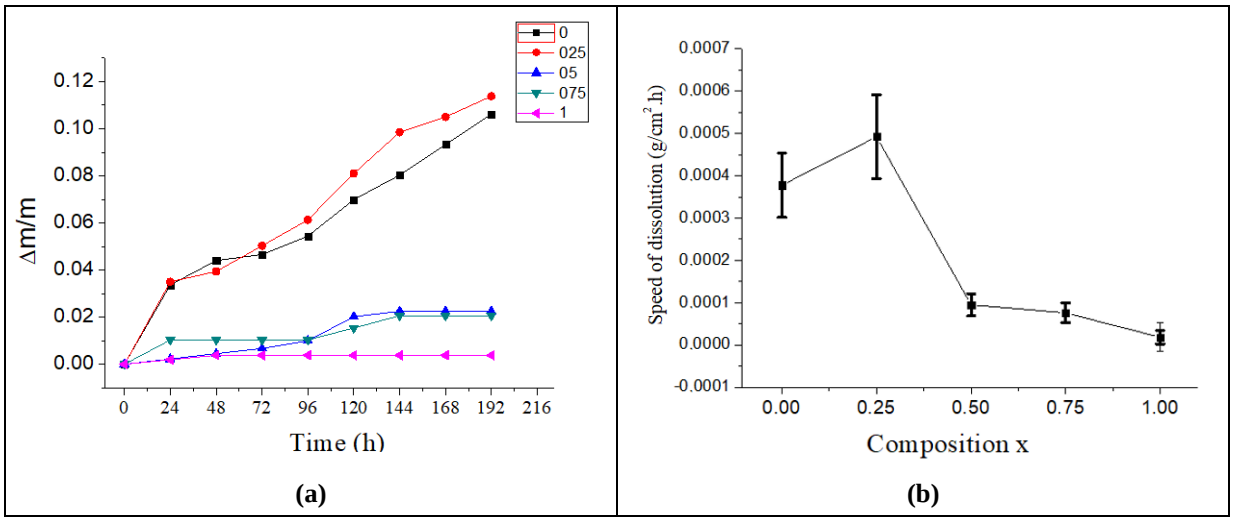

Figure 7. Weight loss in water solution (Δm/m) versus time and dissolution rate ΔR versus NiO content of $37.5Na_2O$-25[(1-x)MgO-xNiO]-$37.5P_2O_5$ ($0 \leq x \leq 1$) glasses.

Conclusion

Phosphate glasses having compositions 37.5Na2O-25[(1-x)MgO-xNiO]-37.5P2O5 (0≤x≤1) were synthesized and investigated to probing the effects on glass structure and properties when substituting Ni^{2+} ions for Mg^{2+} ions. The EPR spectroscopy study reveals an octahedral environment for Ni^{2+} in the glass network. The decrease of molar volume and the increase glass transition temperature versus NiO content implies the reticulation of the glass network due to the replacement of Mg-O bonds by the more covalent Ni-O bonds. These results were confirmed by the increase of the chemical durability.

References

1- J. H. Campbell, T. I. Suratwala, Nd-doped phosphate glasses for high-energy/high-peak-power lasers, J. Non- Cryst. Solids, **2000**, 263-264, 318-341.

2- S. M. Hsu, S. W. Yung, R. K. Brow, W. L. Hsu, C. C. Lu, F. B. Wu, S. H. Ching, Effect of silver concentration on the silver-activated phosphate glass, Mater. Chem. Phys., **2010,** 123, 172-176.

3- C. Chen, R. He, Y. Tan, B. Wang, S. Akhmadaliev, S. Zhou, J. R. Vazquez de Aldana, L. Hu. F. Chen, Optical ridge waveguides in Er^{3+}/Yb^{3+} co-doped phosphate glass produced by ion irradiation combined with femto second laser ablation for guided-wave green and red up conversion emissions, Opt. Mater., **2016,** 51, 185-189.

4- R. K. Brown, D. R. Tallant, Structural design of sealing glasses, J. Non-Cryst. Solids, **1997**, 222, 396-406.

5- V. Salih, K. Franks, M. James, G. W. Hastings, J. C. Knowles, I. Olsen, Development of soluble glasses for biomedical use. Part 2: The biological response of human osteoblast cell lines to phosphate-based soluble glasses, J. Mater. Sci. Mater. Med., **2000,** 11, 615-620.

6- M. Navarro, M. P. Ginebra, J. A. Planell, Cellular response to calcium phosphate glasses with controlled solubility, J. Biomed. Mater. Res., **2003,** 67A, 1009-1015.

7- K. Franks, V. Salih, J. C. Knowles, I. Olsen, The effect of MgO on the solubility behavior and cell proliferation in a quaternary soluble phosphate based glass system, J. Mater. Sci. Mater. Med., **2002,** 13 549-556.

8- R. K. Brow, Review: the structure of simple phosphate glasses, J. Non-Cryst. Solids, **2000,** 263, 1-28.

9- T. Kanazawa, Structural characteristics of MgO-P_2O_5 glasses, J. Non-Cryst. Solids, **1982**, 52, 187-194.

10- H. Schlenz, F. Reinauer, R. Glaum, J. Neuefeind, B. Brendebach, J. Hormes, High-energy X-ray diffraction study of Ni-doped sodium metaphosphate glasses, J. Non-Cryst. Solids, **2005,** 351, 1014-1019.

11- R. Oueslati Omrani, A. Kaoutar, A. El Jazouli, S. Krimi, I. Khattech, M. Jemal, J. J Videau, M. Couzi, Structural and thermochemical properties of sodium magnesium phosphate glasses, J. Alloys Compd., **2015,** 632, 766-771.

12- J. A. Ribeiro, J. Walker, The effects of adenosine triphosphate and adenosine diphosphate on transmission at the rat and frog neuromuscular junctions, Br. J. Pharmacol., **1975**, 54, 213-218.

13- A. Ghosh, P. Ronner, E. Cheong, P. Khalid, F. M. Matschinsky, The role of ATP and free ADP in metabolic coupling during fuel-stimulated insulin release from islet β-cells in the isolated perfused rat pancreas, J. Biol. Chem., **1991**, 266, 22887-22892.

14- A. Thulasiramudu, S. Buddhudu, Optical characterization of Mn^{2+}, Ni^{2+} and Co^{2+} ions

doped zinc-lead borate glasses, J. Quant. Spectrosc. Radiat. Transfer, **2006**, 102, 212-227.

15- L. Gomathi Devi, N. Kottam, B. Narasimha Murthy, S. Girish Kumar, Enhanced photocatalytic activity of transition metal ions Mn^{2+}, Ni^{2+} and Zn^{2+} doped polycrystalline titania for the degradation of aniline blue under UV/solar light, J. Mol. Catal. A: Chem., 2010, 328, 44-52.

16- L. Montagne, G. Palavit, R. Delaval, Effect of ZnO on the properties of (100-x)($NaPO_3$)-xZnO glasses, J. Non-Cryst. Solids, **1998**, 223, 43-47.

17- R. Oueslati Omrani, S. Krimi, J. J. Videau, I. Khattech, A. El Jazouli, M. Jemal, Structural investigations and calorimetric dissolution of manganese phosphate glasses, J. Non-Cryst. Solids, **2014,** 389, 66–71.

18- R. Ait Mouss, S. Krimi, B. Glorieux, I. Khattech, M. Couzi, T. Cardinal, A. El Jazouli, Structural characterization and calorimetric dissolution behavior of Na_2O-CuO-P_2O_5 glasses, J. Non-Cryst. Solids, **2016,** 452, 144-152.

19- R. Oueslati Omrani, S. Krimi, J. J. Videau, I. Khattech, A. El Jazouli, M. Jemal, Structural and thermochemical study of Na_2O-ZnO-P_2O_5 glasses, J. Non-Cryst. Solids, **2014**, 390, 5-12.

20- F. Delahaye, L. Montagne, G. Palavit, P. Baillif, J. C. Touray, Dissolution of (50-x)Na_2O-xCaO-50P_2O_5 metaphosphate glasses in different saline solutions: Mechanism and kinetic control, Glastech. Ber. Glass Sci. Technol., **1999**. 72(5), 161-166.

21- N. Iwamoto, Y. Makino, S. Kasahara, State of Fe^{3+} ion and Fe^{3+}–F^{-} interaction in calcium fluorosilicate glasses, J. Non-Cryst. Solids, **1983**, 55, 113-124.

22- R.P. Sreekanth Chakradhar, G. Sivaramaiah, J. Lakshmana Rao, N.O. Gopal, Fe^{3+} ions in alkali lead tetraborate glasses - an electron paramagnetic resonance and optical study, Spectrochim. Acta, Part A, **2005**, 62, 51–57.

23- R. V. S. S. N. Ravikumar, A. V. Chandrasekhar, L. Ramamoorthy, B. J. Reddy, Y. P. Reddy, J. Yamauchi, P. S. Rao, Spectroscopic studies of transition metal doped sodium phosphate glasses, J. Alloys Compd., **2004**, 364, 176-179.

24- H. B. Premkumar, D. V. Sunitha, H. Nagabhushana, S. C. Sharma, B. M. Nagabhushana, C. Shivakumara, J. L. Rao, R. P. S. Chakradhar, Synthesis, characterization, EPR, photo and thermoluminescence properties of $YAlO_3$: Ni^{2+} nanophosphors, J. Lumin., **2013**, 135,105-112.

25- J. E. Pemberton, L. Latifzadeh, J. P. Fletcher, S. H. Risbud, Raman spectroscopy of calcium phosphate glasses with varying calcium oxide modifier concentrations, Chem. Mater., **1991,** 3, 195-200.

26- G. J. Exarhos, Vibrational studies of glass structure and localized interactions, Chapter 11, In: Structure and bonding in non-crystalline solids, Edited by G. E. Walrafen, A. G. Revez, Plenum Press, New York **1986**, pp. 203- **2017**.

27- A. Rulmont, R. Cahay, M. Liegeois-Duychaerts, P. Tarte, Vibrational spectroscopy of phosphates - some general correlations between structure and spectra, Eur. J. Solid State Inorg. Chem., **1991,** 28, 207-219.

28- C. V. Ramana, A. Ait-Salah, S. Utsunomiya, U. Becker, A. Mauger, F. Gendron, C. M. Julien, Structural characteristics of lithium nickel phosphate studied using analytical electron microscopy and Raman spectroscopy, Chem. Mater., **2006**, 18, 3788-3794.

29- A. de Andres, J. L. Martinez, Vibrational study of R_2BaNiO_5 (R=Y, Ho, Er or Tm), NiO_6 one-dimensional chains, and Tm_2BaNiO_5, NiO_5 pyramids, Solid State Com., **1992**, 82, 931-937.

30- E. Libowitzky, Correlation of O-H stretching frequencies and O-H-O hydrogen bond lengths in minerals, Monatsh. Chem., **1999**, 130, 1047-1059.